Case Studies in Construction Materials 17 (2022) e01601

Contents lists available at ScienceDirect

Case Studies in Construction Materials

journal homepage: www.elsevier.com/locate/cscm

Influence of adding short carbon fibers on the flexural behavior of textile-reinforced concrete one-way slab

Amer M. Ibrahim [a], Suhad M. Abd [a], Omar H. Hussein [a,*], Bassam A. Tayeh [b], ↱Hadee Mohammed Najm [a], Shaker Qaidi [c,d]

[a] Department of Civil Engineering, College of Engineering, University of Diyala, 32001 Diyala, Iraq
[b] Civil Engineering Department, Faculty of Engineering, Islamic University of Gaza, Gaza Strip, ↱Palestine
[c] Department of Civil Engineering, College of Engineering, University of Duhok, 42001 Duhok, Iraq
[d] Department of Civil Engineering, College of Engineering, Nawroz University, 42001 Duhok, Iraq

ARTICLE INFO

Keywords:
Short carbon fibers
Carbon fabric
TRC one-way slab

ABSTRACT

The application of textile reinforcement to the tension zone of the reinforced concrete slabs as a means to enhance flexural capacity has been investigated by researchers in the past. However, the effectiveness of adding short carbon fibers as internal reinforcement in the textile-reinforced concrete one-way slab needs to be studied. The paper presents the experimental research conducted on four full-scale (1500×500×50) mm one-way slabs. An innovative Polyacrylonitrile (PAN) textile grid was used as internal reinforcement in combination with short carbon fibers. The first one consists of fine-grained concrete and short carbon fibers. Two textile-reinforced RC slabs have eight layers of fabric (textile-reinforced concrete (TRC) 8 L) with two percentages of short carbon fiber (0.264% and 0.528%), and one reference textile-reinforced concrete slab without short carbon fiber was fabricated to investigate the flexural behavior under a four-point loading system. The findings indicate that TRC + short carbon fiber showed significantly improved flexural capacity, load-deflection, and load-concrete strain behaviors compared with TRC. The new TRC+ 0.264% short carbon fibers (SCF) and TRC+ 0.528%SCF improved the load-bearing capacity by about 24.19% and 31.56%, respectively, as compared with TRC. Also, the intensity of the crack pattern was measured to compare the ductility of TRC+ short carbon fiber to that of traditional TRC.

1. Introduction

Textile-reinforced concrete (TRC) is a new kind of fiber-reinforced cementitious composite (FRCC). Pakravan, Jamshidi and Rezaei [1] composed of a fine-grained cement-based matrix reinforced by multiaxial textile reinforcement. Engineering applications, utilized Textile reinforced composites for many years. The interest in textile reinforcement was continued since the early 1970 s [2]. The excellent properties of the textile reinforcement encouraged the use of this type of reinforcement instead of conventional steel reinforcement. Textiles are unlike chopped fibers that are distributed randomly in the cementitious matrix. The chopped fibers do not resist the tensile stresses efficiently because of their closely spaced tendency compared to conventional reinforcing bars, however, they are better at controlling the cracking, i.e., these discontinuous fibers can be used as secondary reinforcement.

* Corresponding author.
E-mail address: ekhel199276@gmail.com (O.H. Hussein).

https://doi.org/10.1016/j.cscm.2022.e01601
Received 4 August 2022; Received in revised form 14 October 2022; Accepted 19 October 2022
Available online 20 October 2022

The concrete low tensile strength necessitates the utilization of steel bars with the aim of compensating for the concrete low tensile strength. The sensitivity of the steel reinforcement to corrosion leads to damage to the structural integrity in case of concrete weakness [3]. Due to this steel's corrosive nature, a precautionary thick concrete cover is necessary to overcome this issue regardless of the self-weight excess. The use of stainless-steel bars, fiber-reinforced polymer (FRP) bars, steel and synthetic fibers, epoxy-coated steel bars, and steel welded wire fabric is trying to overcome this issue [4–8].

TRC is a novel composite material made by incorporating continuous textile fabric into fine-grained concrete that consists of a cement binder and fine aggregates. TRC differs from conventional FRC for the reason that it can be positioned where the stresses occur. Papanicolaou and Papantoniou [9] mentioned that the textile reinforcement properties could be fully employed as it is placed in the desired position with sufficient quantity, unlike discrete fibers that are randomly dispersed and oriented. Hence, it is low efficient. Ravindrarajah and Tam [10] found that the presence of fibers in the compression zone has no significant effect on beams. The combination of both Glass Fiber-Reinforced Concrete (GFRC) and ordinary steel-reinforced concrete advantages lead to TRC [11]. Peled and Mobasher [12] stated the superior tensile behavior of alkali resistance (AR) glass fabric composites in terms of strength and toughness as compared with the conventional GFRC.

Generally, more than 3% of short fiber volume fractions are required to reinforce concrete products effectively [2]. Thus, TRC will reduce the cost of structures compared with FRC by employing a reduced volume fraction of fibers. Fig. (1) shows the combination of the steel-reinforced concrete and FRC effects to form the textile-reinforced concrete. However, the TRC presents wide cracks at high deformation [1]. The addition of the discrete fibers to the TRC achieves better cracking control by improving the bridging mechanism [7,8]. The effects of the addition of the short fiber on the TRC's mechanical behavior were studied by various researchers [13–18]. The short fibers exhibit a clear contribution to the load-bearing capacity of the TRC member [19].

However, "the tensile strength, ultimate strength, toughness, and ductility can be quite improved by the addition of short fibers [16, 20–24]. Moreover, the cracking process (initiation, propagation, and widening) is facilitated by such an addition. Thus, the service-ability and durability are improved. Fig. (2) shows the stress-strain behavior for the conventional TRC composite and TRC with short fibers [25]. The TRC with short fibers exhibits higher cracking stress and better strain hardening behavior during the stage of multiple cracking. Hakeem, Amin, Abdelsalam, Tayeh, Althoey and Agwa [26] investigated the flexural behavior of the TRC composites reinforced by both AR glass and PE fabric with 0.1% short PP fibers. The AR glass with short PP fibers showed excellent flexural properties, high strength, and absorbed energy. However, the PE composites did not show such improvement. Yildizel [27] stated the positive effect of the PVA fiber addition on the flexural behavior of the TRC reinforced by carbon fabrics. They concluded that the addition of 1.5% volume content of PVA fibers improved the load-bearing capacity, bond performance, crack control, and deformation more than the 1% volume content of PVA fibers [28] exhibited an identical trend in the composite with AR glass fabrics when short glass fibers (SGF) or SCF are added by 0.5% or 1%, respectively. Fig. (3) shows the stress-strain behavior of the TRC with two types of short fibers. It can be observed that the TRC stress-strain behavior is improved with the addition of each type of short fiber [20,24,29, 30]. However, the tensile strength of the composite was slightly increased while the addition of the short fiber, especially the carbon, extended the strain capacity in the multiple cracking stages. While the conventional TRC showed no such extension, Zeyad, Khan and Tayeh [31] classified the short AR glass fibers added to the TRC composite into two types: dispersed and integral (Fig. 4). They studied the effects of the two types of short AR glass fibers. The TRC with short, dispersed fibers exhibited higher cracking stress and achieved strain region expansion at the multiple cracking stages. In contrast, the short integral AR fibers slightly improved the first crack stress. However, the tensile strength of the composite and the work to fracture are improved with the two types of fibers [20,32–35]. The variations between the dispersed and integral fibers are attributed to the bond nature between each fiber type and the matrix. The connection between the matrix and an individual fiber is perfect in the case of short, dispersed fibers. While only the sleeve filaments are in good contact with the matrix in the case of integral fibers due to their bundled nature, the inner fibers showed sliding versus each

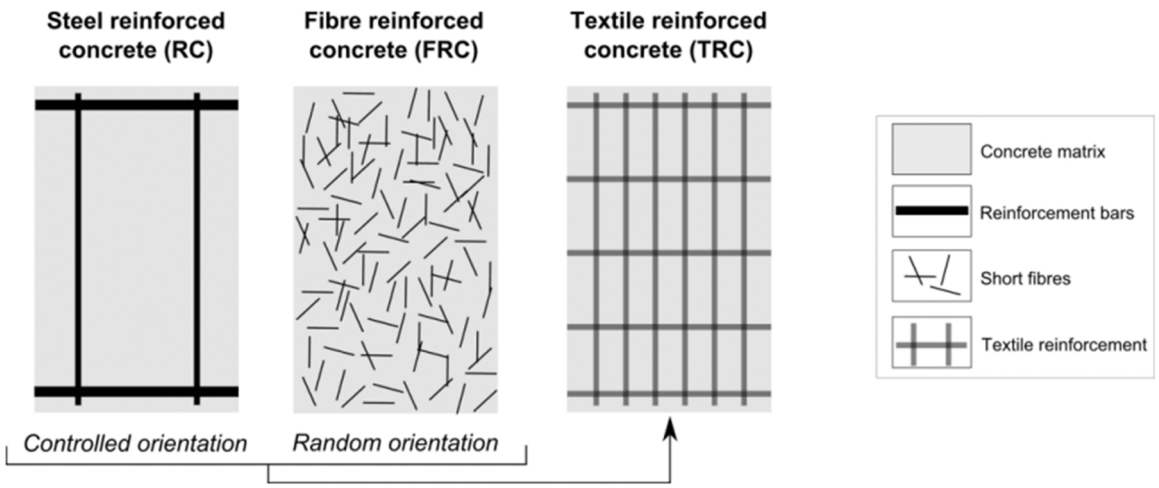

Fig. 1. : Combined effects of RC and FRC forming TRC.

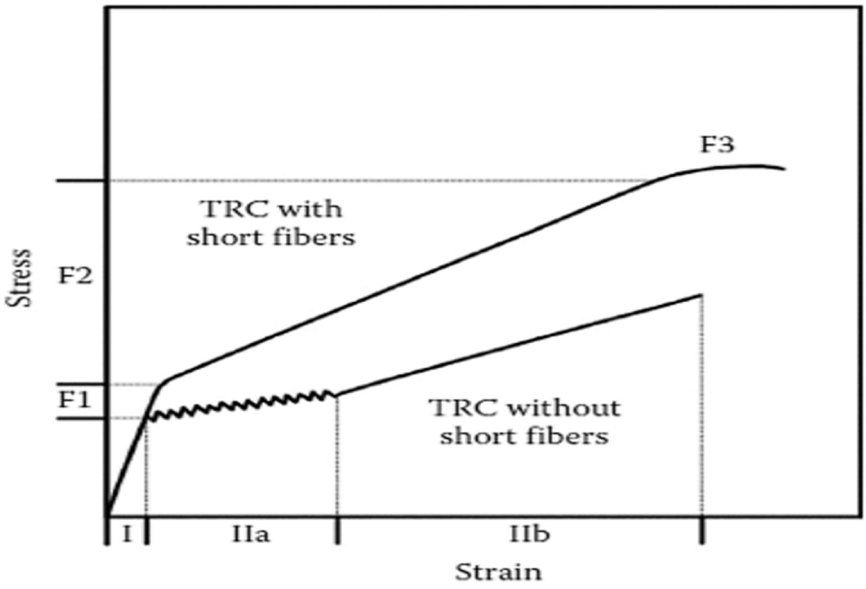

Fig. 2. : Schematic description of the influence of the addition of short fibers to TRC on the stress-strain response [28].

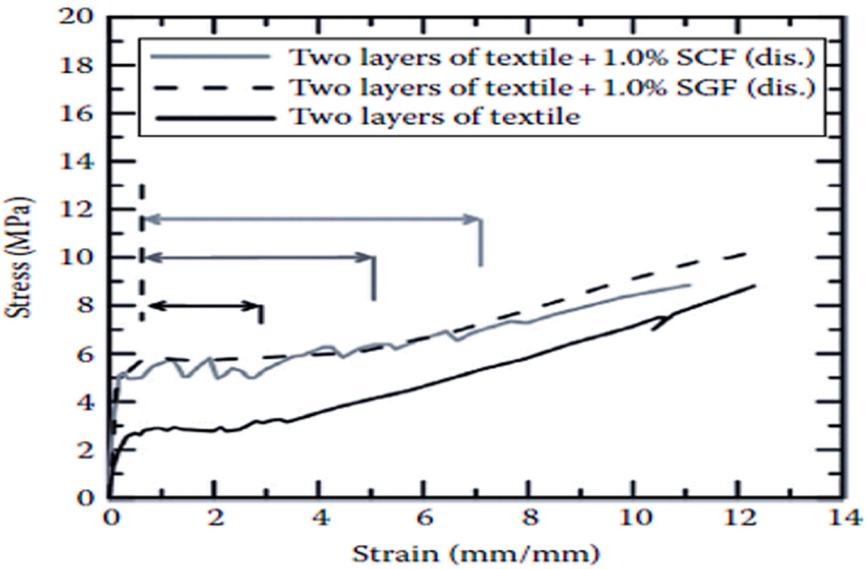

Fig. 3. : Tensile response of AR glass TRC with short fibers of glass (SGF) or carbon (SCF) and without short fibers [28].

other during loading. Subsequently, the sleeve fibers are mainly activated at low deformations, while the core fibers are exclusively activated at extreme deformations [32]. The addition of short fibers is adopted based on the various essential mechanisms that explain the improvement in the mechanical properties of the TRC: The short fibers do four things: (1) the short fibers prevent the growth of the fine cracks and restrain their propagation by bridging the micro-cracks; (2) the matrix shrinkage and the damage of internal matrix may be restrained by the addition of short fibers; (3) the inclusive reinforcement degree is raised; and (4) the short fibers work as cross-links that enhance the bond between the fabric yarn and the matrix [21,22,32]. Additionally, there are some ways to improve the impregnation of the mesh of TRC by the use of the rheological active microfibers as mentioned in these previous studies" [36–43].

This study aims to investigate the effects of the addition of short carbon fibers on the flexural behavior of the TRC one-way slab reinforced by carbon fabric layers. The comparison between the contribution of the short carbon fibers individually and with the carbon fabric.

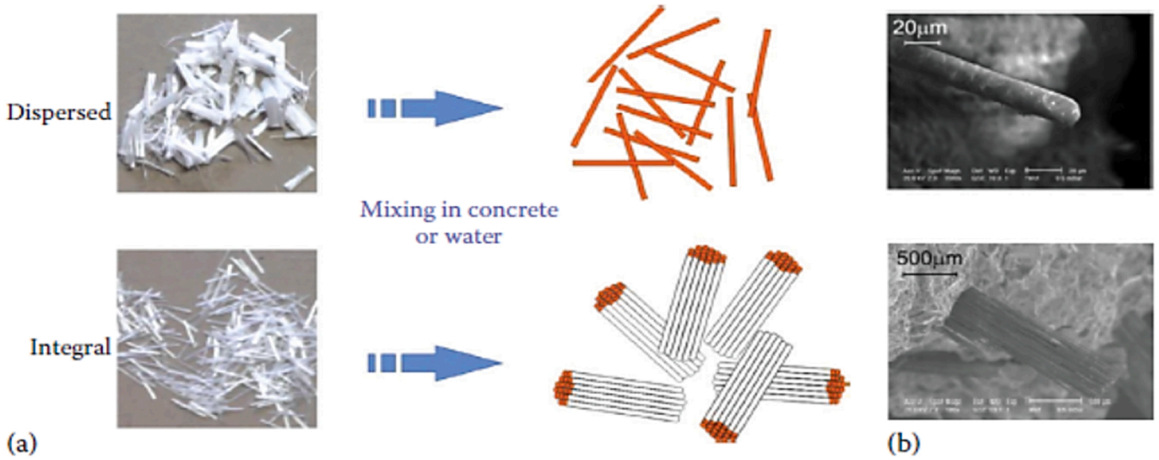

Fig. 4. : (a) Images and graphic representations of dispersed versus integral short fibers and (b) ESEM images of the fibers [14].

2. Materials and methods

2.1. Concrete matrix

The three mixes used in this study are: "the main mix, which is the cementitious matrix or the mortar that is composed of ordinary Portland cement, fine sand with a grading size of 150–600 μm, silica fume (micro silica) used as an addition, and superplasticizer, which is a hydrous solution of modified polycarboxylate basis. Table 1 illustrates the matrix constituents. The other two mixes are the same mortar mix with 0.25% and 0.5% vol of short carbon fibers, respectively. The compression tests were done after completion of the curing duration for 7 and 28 days in order to gain the mortar matrix compressive strength. Thus, six cylinders with dimensions of 100 × 200 mm were used, the first three (100 ×200 mm) cylinders were tested at 7 days while the other cylinders were tested at 28 days. The compressive strength test (f′c) was carried out according to ASTM C39. The cylinders were loaded axially using a MATEST testing; Machine with 2000 kN capacity. Table (2) illustrates the mechanical properties of the three mixes" [44].

2.2. Textile reinforcement fabrics

One type of textile reinforcement used in this study is "the dry carbon fiber mesh (PAN) as shown in Fig. (5(a and b)) with a looping size of (2.5 ×3) cm and 12k filament. This type of reinforcement was supplied by (JIAXING NEWTEX COMPOSITES); Table (3) shows the manufacturer data sheet. Fig. (6) shows the reinforcement details for the conventional TRC and TRC with short carbon fibers" [44].

2.3. SCF

Short, discrete, discontinuous carbon fibers with a length of 8 mm were dispersed in the concrete mix during mixing. The short carbon fibers are added in two different volumetric ratios (0.528% and 0.264%) to the cementitious matrix during the mixing. The short carbon fibers are added to the three one-way slabs, which are the FRC and one TRC 8 L slab by a 0.528% volume fraction, and the other TRC 8 L slab with a 0.264% volume fraction. Because the short fibers are randomly distributed in the concrete mix, their random distribution and orientation have a significant influence on the strength capacity of the FRC and TRC specimens. Table (4) illustrates the properties of the short carbon fibers. Fig. 7 shows the short carbon fibers.

2.4. Sample preparation

The plywood molds with dimensions of 1500 × 500 × 50 mm are "used for casting the four slab specimens. Firstly, the molds were

Table 1
Constituents of The Fine-Grained Concrete [44].

"Cement kg/m^3	650
Silica fume kg/m^3	65
Sand (0–0.6) mm kg/m^3	1215
Superplasticizer kg/m^3	15.37
water Kg/m^3	250
Cylinder compressive strength (28) day MPa	45
Flow ability, diameter in cm	25″

Table 2
The mechanical properties of the concrete mixes [44].

Type of concrete mix	Cylinder compressive strength MPa (28days)	Splitting tensile strength MPa (28 Days)	Flexural strength MPa (28 days)
Mortar (TRC)	45	4.29	6.05
FRC 0.264%V_f	53.6	4.48	8.42
FRC 0.528%V_f	56.3	4.67	10.26

a) one layer in the plywood mold b) carbon fabric Roll

Fig. 5. (a and b): Carbon fabric reinforcements.

Table 3
Properties of textile reinforcement provided by the manufacturer [44].

"Material	12k carbon fiber
Weight (g/m^2)	160 ± 10 (g)
Width (cm)	100
Thickness (mm)	0.2
Mesh size (cm)	2.5 × 3
Tensile strength (MPa)	3530
Tensile modulus (GPa)	230
Colour	Black"

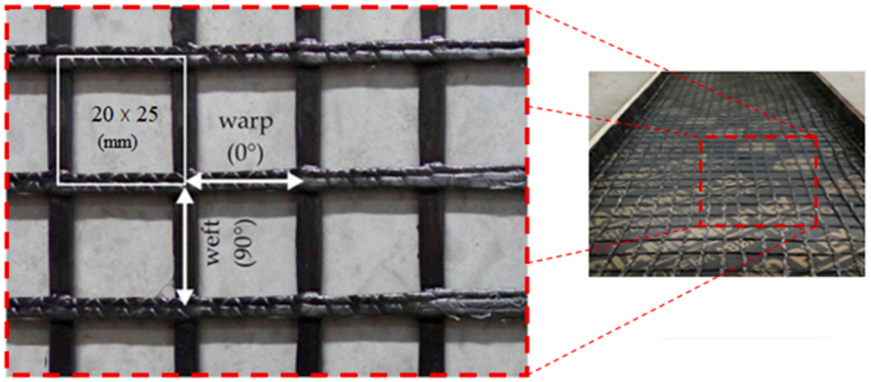

Fig. 6. Details of the slab specimen TRC and TRC+ short carbon fibers.

Table 4
Properties of the short carbon fibers [44].

"Fiber length	8 mm
Diameter	7± 2 μm
Aspect ratio	1140
Tensile strength	3.5 GPa
Young's modulus	230 GPa
Density	1.8 g/cm^3
Chemical resistance	High
Absorption	Nil"

Fig. 7. Short carbon fibers.

oiled in order to inhibit the adhering of the concrete on the mold interior walls. For the FRC specimen, the cementitious matrix that contained 0.528% short carbon fibers was poured directly. While the other three specimens are cast in sequential processes as follows: The little amount of concrete was poured for 4 mm, then the first three layers were sequentially placed with some squeezing for each layer applied by the hand leveling instrument to enhance the penetration of the concrete matrix through the fabric openings, particularly with 4 mm concrete cover and accumulation of fabric layers. The delamination chance is increased; hence this compaction method is achieved to inhibit the delamination occurrence and to assure the fabric layers' levelness. Another concrete amount is cast to a 10 mm thickness, where the second three layers were laid; thereafter, the last two layers were placed at a 15 mm concrete thickness. The slight tension is applied by hand from both layers' opposite ends in order to keep the straightness and orientation of the layers. The specimens were demolded after 24 h and cured in a water curing basin at 23 °C. The slab specimens were removed from curing and dried, painted, and fixed with the strain gauges on their surfaces in order to perform the four-point bending test after 28 days" [44]. Fig. (8(a, b, c, and d)) shows the casting processes.

2.5. Instrumentation and measurements

2.5.1. Deflection measurement devices

Three dial gauges were used to "measure the vertical deflection (displacement) of the tested slab specimens. One was at the mid-span and the other two gauges were placed below the center of the distance between the support and the loading point. These dial gauges are differentiated by their types, capacity, and accuracy. The electronic dial gauge has a capacity of 25.4 mm and a 0.01 accuracy, while the others are mechanical dial gauges with a capacity of 30–50 mm and an accuracy of 0.01 mm. The deflection values obtained from the three gauges were directly recorded for each applied load" [44].

2.5.2. Strain measurement device

Strains were measured to "determine the behavior of the one-way slab specimens against the applied stress. The use of a highly accurate device is required to calculate the amount of strain in the concrete. The BF120–20AA strain gauge type produced by the SNC company was used to measure the compression strain of concrete during the test. Table (5) shows the properties of this strain gauge type. The strain gauges were fixed on the concrete surface for each specimen and connected to the TDS-530 data logger device (Fig. 9). The concrete strain values were saved and printed for each load" [44].

Fig. 8. (a, b, c, and d)): The main casting processes.

Table 5
Strain Gauge Properties [44].

"Gauge type	Resistance in Ω	Grid size (mm)	Gauge dimensions	
			Length (mm)	Width (mm)
BF120–20AA	120	20 × 3.5	25	5″

2.5.3. Four-point bending test

The flexural test is considered the primary test which evaluates the bending capacity and ductility of the TRC-RC one-way slab. Four-point bending tests were executed to "investigate the bending capacity of the three slab specimens. The slabs were tested after 28 days. They were prepared, cleaned, and coated with a white colour in order to reveal possible cracks. The slabs are simply supported over a clear span of 1400 mm and are tested under two concentrated loads applied at 550 mm from each support. The load is applied, and the strain and deflection readings are taken every 0.11 kN. At each increment, manual measurements are recorded, including the applied load, deflection, crack width, and textile, steel, and concrete strains. A hydraulic universal testing machine is a machine having a maximum range capacity of 600 kN used for testing slab specimens. The test was done in the structural laboratory of the civil department in the college of engineering at Diyala University. Fig. (10) shows the four-point bending test" [44].

3. Results and discussion

3.1. Contribution of the short carbon fibers

This section discusses the contribution of the textile reinforcements and short carbon fibers to the flexural capacity of the four tested slabs. Table (6) and Fig. 11 shows the test results for the four tested slabs. It can be observed that the carbon fabric reinforcements yield a higher contribution to the load-bearing capacity than the short carbon fibers with a similar volume fraction. The contribution of the carbon fabric reinforcement in the TRC 8 L slab was equal to 8.7 times that of the short carbon fibers in the FRC slab. However, this premium contribution achieved by the carbon fabric reinforcement is explained by the continuity of the fibers in the form of yarns and

Fig. 9. : TDS-530 Data logger used in this work.

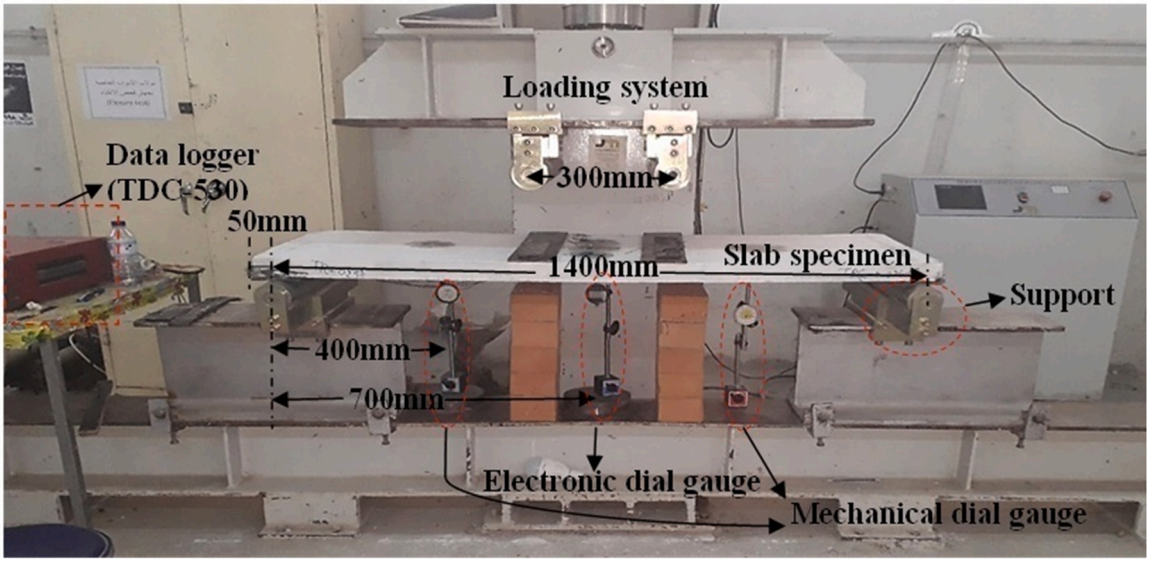

Fig. 10. : Four-Point Bending Test.

Table 6
Test results for the four tested slabs.

Slab symbol	Area mm^2	$\%V_T$	$\%V_{CF}$	First crack strength MPa	Ultimate flexural strength MPa	% Contribution of carbon fabric layers	% Contribution of short carbon fibers
FRC	–	–	0.528	6.6	6.6	–	8.3
TRC 8 L	72	0.528	–	7	22.04	72.5	–
TRC+ 0.264% SCF			0.264	6.76	27.38	77.9	5.4
TRC+ 0.528% SCF			0.528	6.96	29	79.1	6.6

filaments while the short fibers are dispersed randomly in the matrix. This continuity leads to a higher aspect ratio and better utilization. Furthermore, the orientation of the fibers has a great effect on its behavior. Consequently, the carbon fabric orientation can be easily controlled rather than the randomly oriented short fibers [23,24,29,30]. From the comparison between the contributions of the

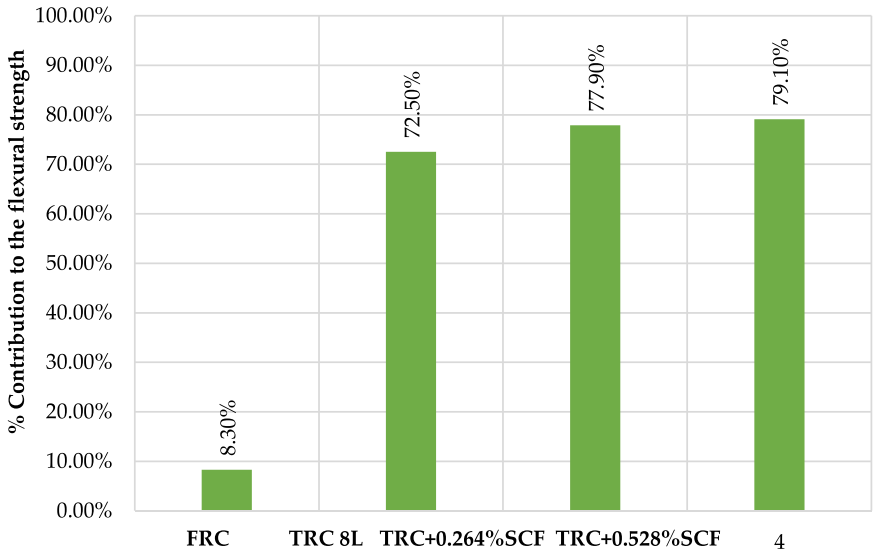

Fig. 11. Contribution Percentages for The Four Tested Slabs.

short carbon fibers in both FRC and TRC+ 0.528%SCF, it can be noticed that the contribution of the short carbon fibers is reduced by 20.8% in the last. This reduction can be interpreted by the random distribution of the short carbon fibers and its accumulation in some zones rather than others. Also, as shown in Fig. 7, the nature of short fibers, which are integral, may contribute to this limited improvement. However, the TRC+ 0.264%SCF exhibited a 65% fibers contribution that in the FRC. Accordingly, this percentage of the short carbon fibers contribution seems to be perfect as compared with the 100% short fiber addition. Moreover, the addition of the short carbon fibers by 50% and 100% from volume fraction leads to an increase in the ultimate flexural strength by 24.42% and 31.6%. This agrees with Pakravan, Jamshidi and Rezaei [1] who mentioned that the addition of short fibers increased the flexural strength of Hyb-TRC by up to 9.14%.

3.2. Load-deflection behavior

The load-deflection behavior of the textile-reinforced concrete is typically nonlinear, however, this behavior is divided into three stages: the initial is linear elastic since the concrete is uncracked, and the textile reinforcements have a negligible contribution to the strength during this stage. The pursue nonlinear stage is initiated by the first crack formation which is accompanied by the transformation of the tensile stresses from the concrete matrix to the textile reinforcement, and the redistribution of the stresses takes place that causes continuous cracks occurrence. The last stage is clarified by the brittle failure of the textile reinforcements when the strain passes the ultimate tensile strain.

Table (7) demonstrates the test results for the four tested slabs. The cracking load is increased for the TRC 8 L by 6% as compared with the FRC cracking load, while both TRC+ 0.264% SCF and TRC+ 0.528% SCF showed a reduction in a load of cracking by 3.4% and 0.57% respectively as compared with the TRC 8 L. However, this reduction is trivial while it is expected that the addition of the short fibers in any amount leads to an increase in a load of cracking. This is in agreement with Du, Zhang, Liu, Zhou, Zhu and Pan [45] who stated that the crack resistance of the specimens and the first crack stress were increased since the matrix improved with steel fibers. The nature of short carbon fibers is responsible for the lack of improvement in the cracking load. The cracking load of the FRC is identical to its ultimate load since the brittle failure immediately occurs beyond the first crack. This is due to the random distribution of the short carbon fibers, which constricts their utilization in the zones where the tensile stresses occur. The addition of the short carbon fibers to the carbon fabric layers in the two TRC+ 0.264% SCF and TRC+ 0.528% SCF slab specimens exhibit an increase in the load-bearing capacity by about 24.19% and 31.56% respectively as compared to the TRC 8 L. This corresponds to Pakravan, Jamshidi and Rezaei [1], Pakravan and Ozbakkaloglu [46], who concluded that the Hyb-TTRC samples with the addition of short PVA fiber to the matrix lead to better load-bearing capacity under flexural loading after peak load as compared with the Hyb-TRC sample. The

Table 7
The test results for the four tested slabs.

Slab symbol	First crack load kN	Ultimate load kN	Mid-span Deflection mm
FRC	5	5	2.06
TRC 8 L	5.3	16.7	46.34
TRC+ 0.264%SCF	5.12	20.74	38.78
TRC+ 0.528%SCF	5.27	21.97	40.8

improvement in the load-bearing capacity is attributed to the enhancement in the bond between the carbon fabric layers and the cementitious matrix, which is achieved by the addition of the short fiber [47,48]. The ultimate deflection at the mid-span is highly increased in the three TRC 8 L, TRC + 0.264% SCF, and TRC + 0.528% SCF as compared with the FRC deflection. However, the mid-span deflection at the ultimate load is reduced for the TRC+ 0.264% SCF and TRC+ 0.528% SCF by about 16.31% and 11.96% respectively as compared to the TRC 8 L mid-span deflection. This is attributed to the higher post-cracking stiffness that the TRC+ 0.264% SCF and TRC+ 0.528% SCF yield in terms of the bond improvement and inhibition of the core filament slippage.

Fig. (12) shows the load-deflection curves for the four tested slabs. It can be noticed that the four slab curves are identical from the load initiation till the cracking. FRC showed linear elastic behavior till the failure, while the other three slabs' curves continued beyond the cracking. The cracking point represents an inflection point at which the behavior is transformed from uncracked linear elastic to cracked nonlinear behavior. The tensile stresses are directly transferred from the cracked concrete to the reinforcement at this zone. The continuity of the carbon fabric reinforcement plays a vital role in the continuity of stress redistribution. Therefore, the continuous fabric reinforcement achieves the clear strain hardening behavior that is clarified by multiple cracking formations. The TRC+ 0.264% SCF and TRC+ 0.528% SCF yield lower deflection as compared with the TRC 8 L at the same load. This confirms the improvement in the post-cracking stiffness that the addition of the short carbon fibers achieves. This is confirmed by Du, Zhang, Liu, Zhou, Zhu and Pan [45], who declared that the load-deflection curve became smoother with the increase in the steel fibers in the specimen. The bond improvement realized by the addition of the short carbon fibers clarifies this enhancement in flexural stiffness. Furthermore, the tension stiffening is perfectly improved with the addition of the short fiber, and this is clearly observed during the tests when the new cracks form in the zone between two primary cracks. However, the occurrence of this phenomenon is mainly related to the bond between the reinforcement and the concrete [49,50].

3.3. Strain of the concrete in the compression zone

This section discusses the load-strain behavior of the top concrete in the four tested slabs. As can be observed in Table 8, the concrete compressive strain showed similar values for the FRC at the cracking and failure. However, the concrete cracking strain for the latter is equal to 61% of the TRC 8 L cracking strain. This confirms the excellent contribution of the fabric reinforcement in bearing the tensile stresses during the uncracked stage and delaying the earlier cracking. The concrete compressive strain for the TRC+ 0.264% SCF and TRC+ 0.528% SCF was reduced by 8.43% and 14.29%, respectively, as compared with the TRC 8 L. This may be attributed to the random dispersion of the short carbon fibers that leads to a limit on the contact between the fabric reinforcement and the matrix. However, the ultimate concrete strain is increased for the latter two slabs by 10.2% and 33.1%, respectively, as compared with TRC 8 L. This is confirmed by Barhum and Mechtcherine [51], who states that the strain region is expanded by adding the short-dispersed fibers. This strain extension especially takes place in the region between the first crack occurrence and the end of multiple cracking.

Fig. 13 shows the load-strain curves for the concrete in the four tested slabs. As can be noticed, the four curves are identical to each other during the uncracked region. However, the FRC behavior is terminated by cracking. At the same load, the TRC 8 L exhibits greater concrete strain than the TRC+ 0.264% SCF and TRC+ 0.528% SCF. However, the latter two slabs exhibit identical load-strain behavior until the TRC+ 0.264% SCF failure, which is followed by the TRC+ 0.528% SCF failure.

Figs. 14, 15, 16, and 17 show the deflection profiles for the four tested slabs. It can be observed that the FRC yields lower rotation as compared with the other three slabs. The TRC+ 0.264% SCF and TRC+ 0.528% SCF show lower rotation as compared with the TRC 8 L at a similar load. However, the rotation is rapidly increased for the TRC 8 L after 7.3 kN, TRC+ 0.264% SCF after 8.97 kN, and for the TRC+ 0.528% SCF beyond 15 kN. This confirms the improvement in the flexural stiffness that delays the rapid rotation occurrence [52].

3.4. Toughness and deformability

3.4.1. Toughness

The material toughness can be defined as the material's ability to absorb energy in the plastic zone up to rupture. The determination process of the material toughness consists of calculating the total area which is bounded by the force-deformation curve or the stress-strain curve with respect to the tested sample volume. This area indicates the energy amount per unit volume, which the material can acquire till the rupture. Table (9) illustrates the toughness values for three tested slabs. As can be observed, the toughness increases for the TRC+ 0.25%SCF and TRC+ 0.5%SCF by about 7.7% and 25.9%, respectively, as compared with the TRC 8 L toughness. This is in agreement with Du, Zhang, Liu, Zhou, Zhu and Pan [45], who stated that the addition of steel fibers to the TRC improved the interfacial bonding performance between textile and matrix and increased the flexural toughness. Fig. (18) shows the toughness values for the three tested slabs.

3.4.2. Deformability

The Canadian Standards Association [53] developed a method to "estimate the ductility performance of concrete members that are reinforced by brittle reinforcement materials. However, this method accounted for both strength and deflection factors. The strength factor represents the ratio of the ultimate load to a load of 0.001 concrete compressive strain. The deflection factor is the ratio of the ultimate mid-span deflection to the member mid-span deflection at this concrete strain. Generally, the CAN/CSA S-806 12 replaced the moment with the load since the moment is a function of load and span and the curvature by the deflection since both of them represent a function of loads, spans, and stiffness. In any case, this performance factor must be greater than 4 for rectangular sections and greater than 6 for T-sections" [44]. The deformability factor is calculated as follows:

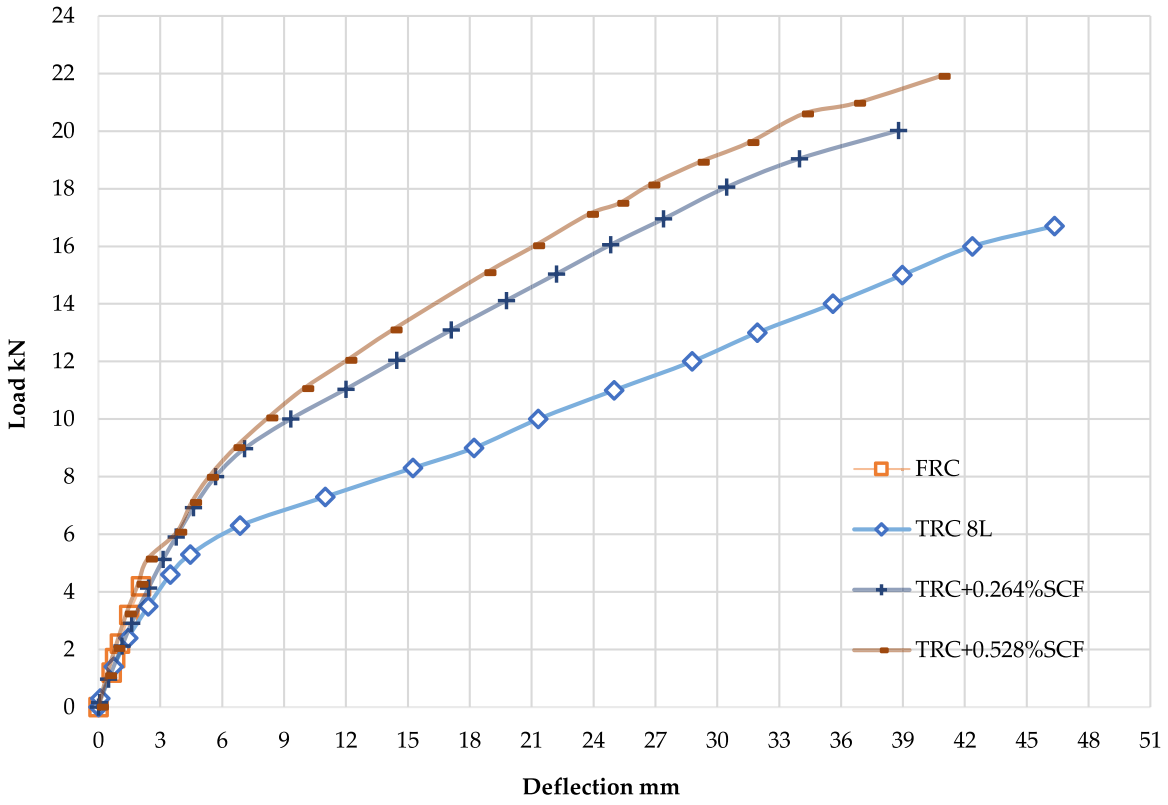

Fig. 12. : The load-deflection curves for the four tested slabs.

Table 8
Compressive strain for the concrete in the four tested slabs.

Slab symbol	The top face of concrete	
	ε_{cr}	ε_{u}
FRC	0.000261	0.000261
TRC 8 L	0.000427	0.002188
TRC+ 0.264% SCF	0.000391	0.002411
TRC+ 0.528% SCF	0.000366	0.002912

Deformability factor = strength factor × deflection factor

$$\text{Strength factor} = \frac{\text{Pu}}{\text{P0.001}} \tag{1}$$

$$\text{Deflection factor} = \frac{\Delta u}{\Delta 0.\quad 001} \tag{2}$$

Table (10) shows the deformability values for the three tested slabs. As can be noticed that the deformability increases for the TRC+ 0.25%SCF, and TRC+ 0.5%SCF by about 29.4%and 36.31% respectively as compared with the TRC 8 L tested slab. Despite that, the ratio of the ultimate load to the 0.001 mortar strain load for both the TRC+ 0.25%SCF and TRC+ 0.5%SCF is perfectly within the TRC 8 L value, while the deflection ratio is higher. This is attributed to the lower deflection that both TRC+ 0.25%SCF, and TRC+ 0.5%SCF yield at the 0.001 mortar strains as compared with TRC 8 L deflection at this moment. Fig. (19) shows the deformability of the three tested slabs.

3.5. Cracks number, width, and spacing for tested group

Table (11) demonstrates the crack details for the three tested slabs. It is noticed that the first crack load represents 31.74%, 24.87%, and 23.99% of the ultimate load for the TRC 8 L, TRC+ 0.25%SCF, and TRC+ 0.5%SCF respectively. The reduction in percent for both

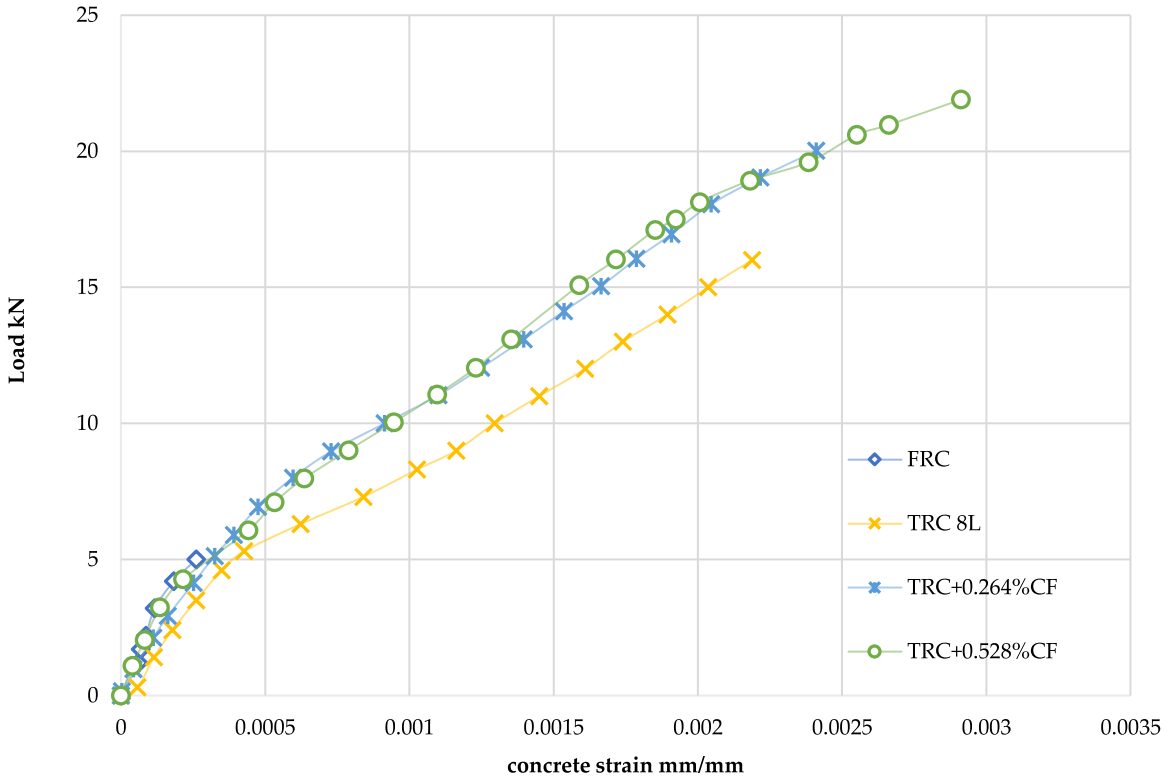

Fig. 13. : Load-compressive strain curves for the concrete in the four tested slabs.

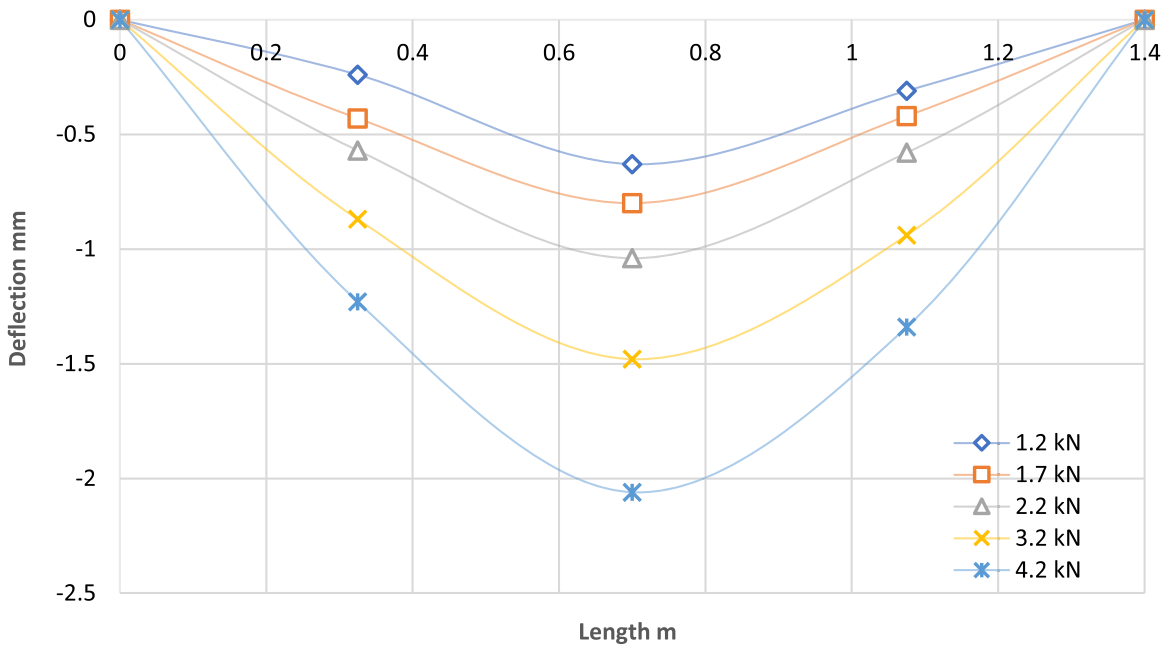

Fig. 14. : Deflection profile for the FRC-tested slab.

TRC+ 0.25%SCF and TRC+ 0.5%SCF is imputed to the ultimate load increase in both of them. The table also shows the reduction in the number of cracks for the last two specimens, which is attributed to the bridging mechanism of the dispersed carbon fibers that inhibits the initiation of the micro-cracks. Also, it can be noticed that the spacing between the cracks increases gradually as the percentage of additional chopped fibers is increased. This is confirmed by Du, Zhang, Liu, Zhou, Zhu and Pan [45], who mentioned that

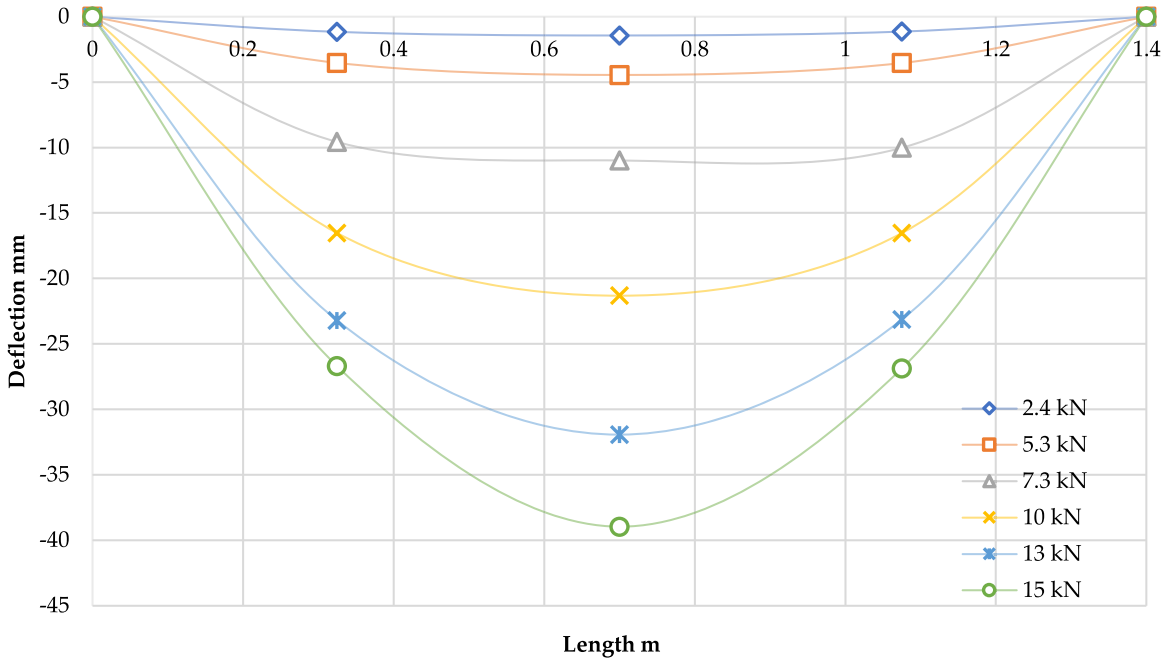

Fig. 15. : Deflection profile for the TRC 8 L tested slab.

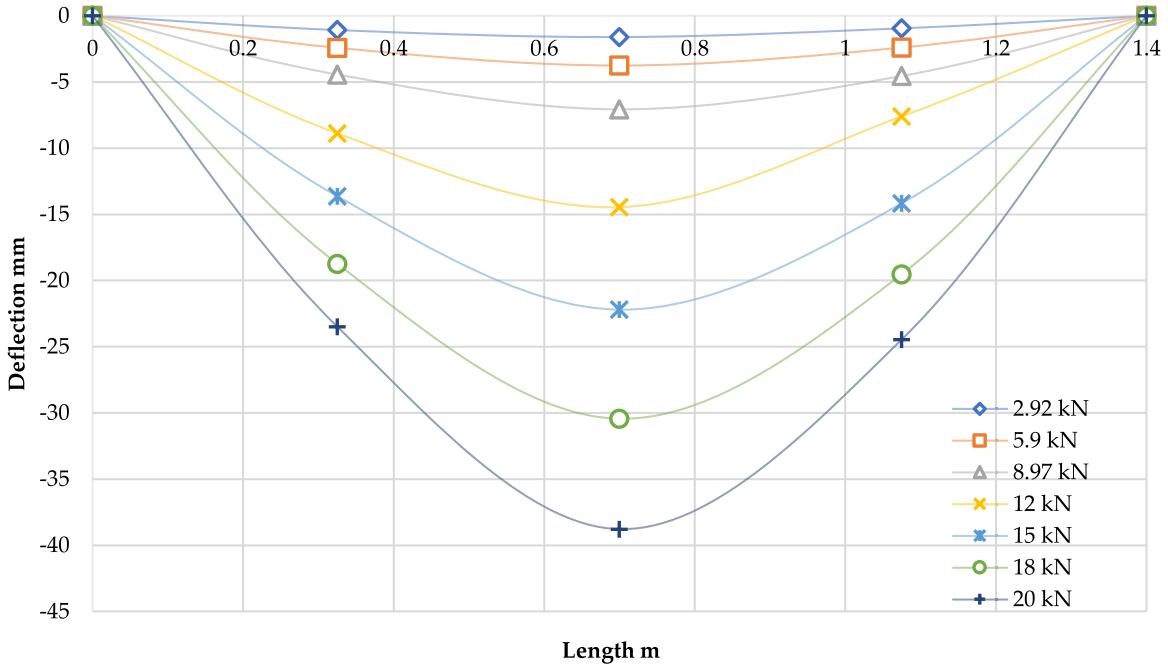

Fig. 16. : Deflection profile for the TRC+ 0.264%SCF tested slab.

the number of cracks increases and the average spacing between the cracks reduces with the increase of steel fiber content. On the other hand, Pakravan, Jamshidi and Rezaei [1] stated that the addition of short PVA fibers to the cement mixture increased the number of cracks on the Hyb-TRC, and the formation of multiple micro-cracks can enable better energy absorption of the composite and contribute to higher fracture resistance by preventing crack localization. The horizontal cracks occurred in the last two specimens with a higher number in the TRC+ 0.5%SCF with respect to TRC+ 0.25%SCF. Most of these cracks took place in the bending region at the load 16–17 kN, while there are two cracks in the TRC+ 0.5%SCF taking place in the shear zone.

Furthermore, the horizontal cracks that form at the neutral axis in the last two slabs are the reason for the bond weakness. The first

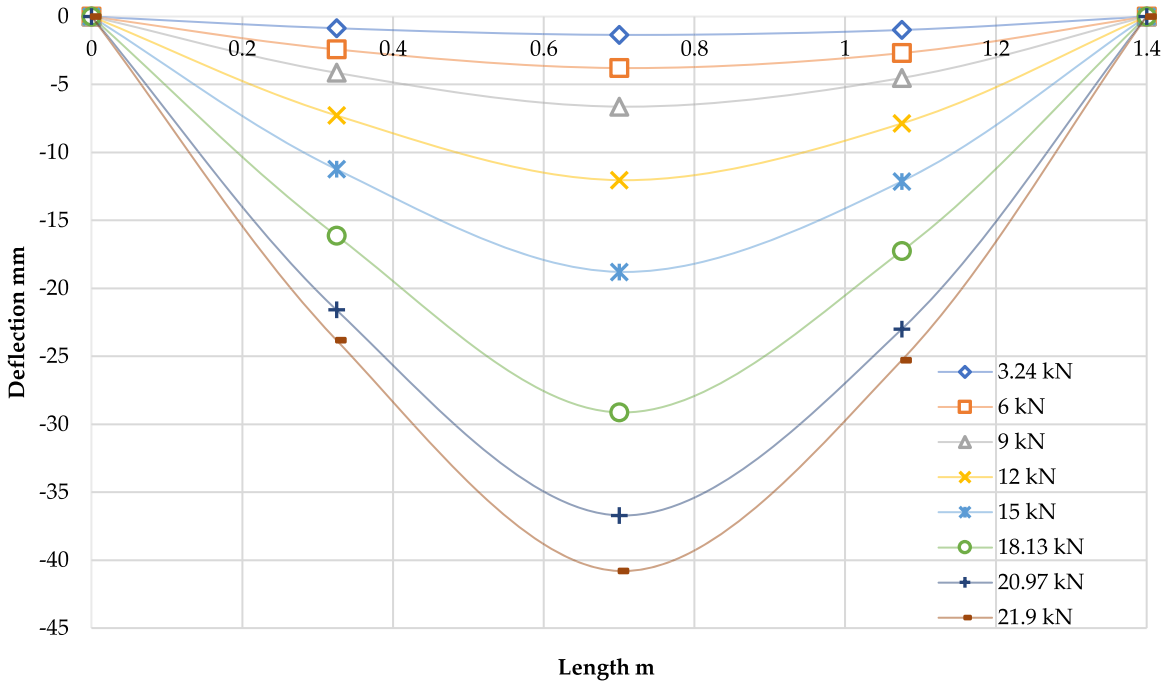

Fig. 17. : Deflection profile for the TRC+ 0.528%SCF tested slab.

Table 9
Toughness for group four slabs by two methods.

Slab symbol	Member toughness (N.mm/mm^3)			Difference %
	Method 1	Method 2		
		($\int_0^{\Delta u}$ **2nd**.eq)	R^2	
TRC 8 L	0.01284889	0.01272952	0.9735	-0.938
TRC+ 0.25% SCF	0.01376228	0.013709253	0.9768	-0.387
TRC+ 0.5% SCF	0.01605332	0.016026933	0.9839	-0.165

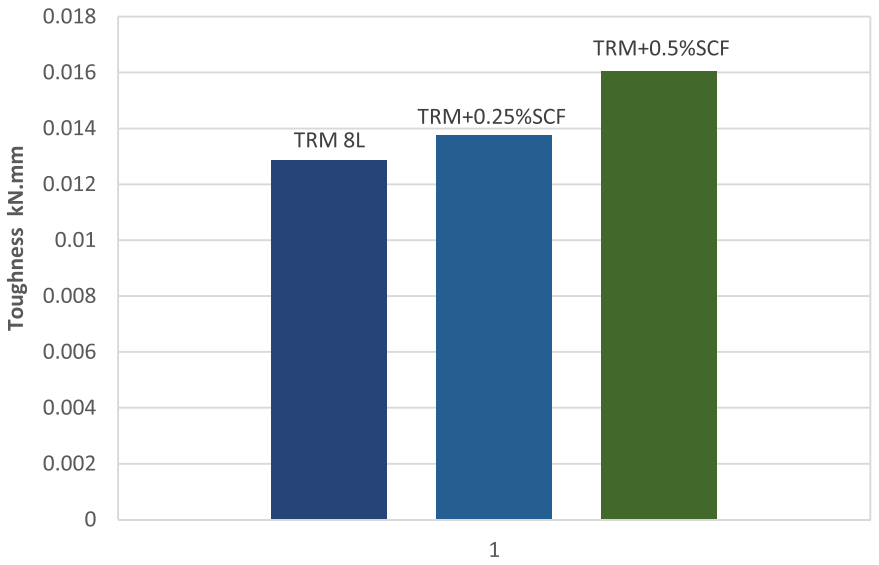

Fig. 18. : Toughness for group four slabs.

Table 10
Deformability for group four slabs [44].

Slab symbol	Strength factor	Deflection factor	Deformability
TRC 8 L	1.93	2.78	5.37
TRC+ 0.25% SCF	1.91	3.64	6.95
TRC+ 0.5% SCF	1.92	3.81	7.32

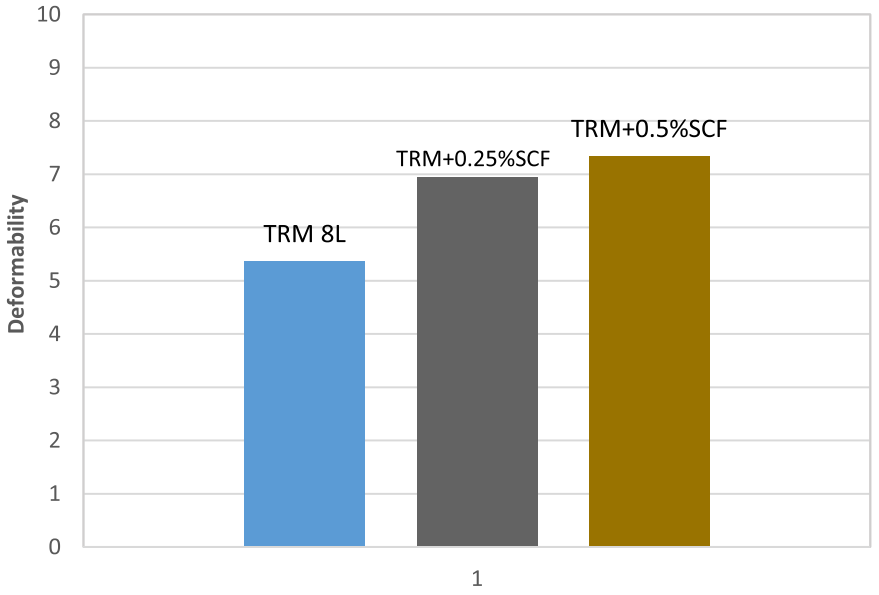

Fig. 19. : Deformability for group four slabs.

Table 11
Cracks details for group four slabs.

Slab symbol	First crack load kN	% $\frac{F.C}{Pu}$	No of V cracks	No of H cracks	First crack width mm	Crack width at ultimate load mm	Spacing cm	
							S_{min}	S_{max}
TRC 8 L	5.3	31.74	40	–	0.02	0.1	1	3
TRC+ 0.25% SCF	5.12	24.87	29	3	0.02	0.14	2	4
TRC+ 0.5% SCF	5.27	23.99	26	8	0.02	0.12	3	5

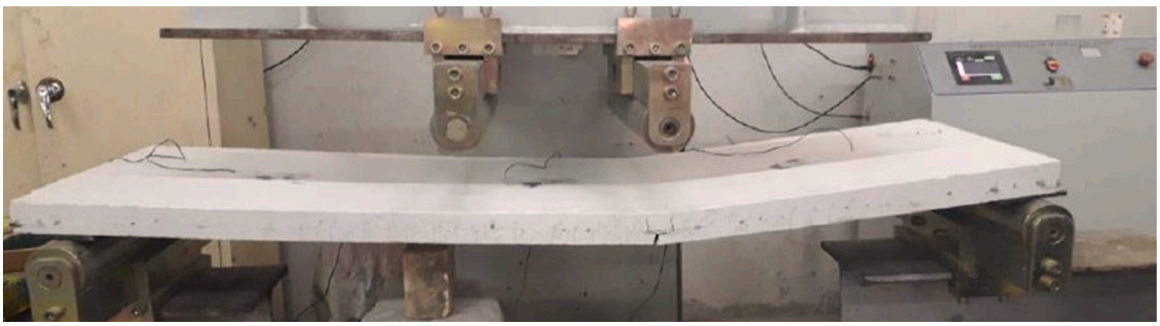

Fig. 20. Cracks details for the TRC 8 L.

Fig. 21. Cracks details for the TRC+ 0.25%SCF.

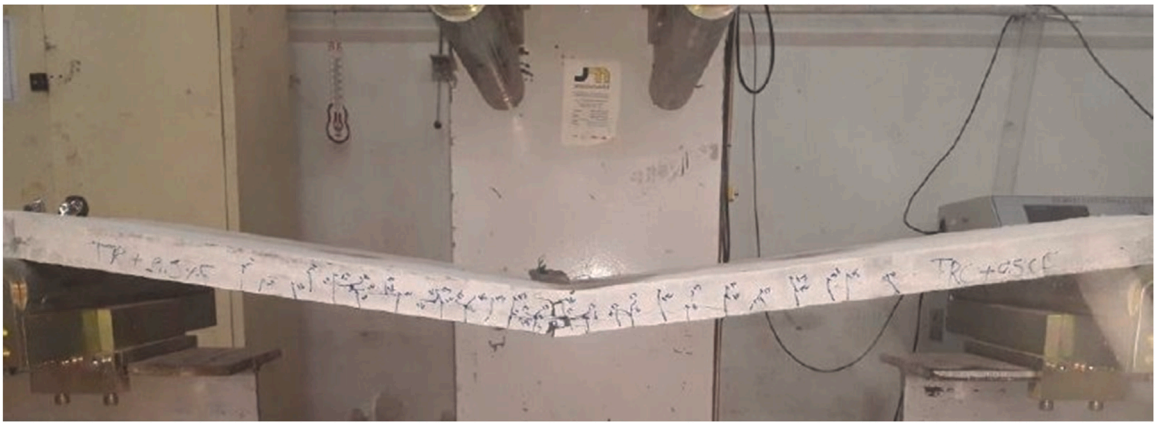

Fig. 22. : Cracks details for the TRC+ 0.5%SCF.

crack initiates with the same width for the three slabs. However, the crack width at the final stage is increased by about 40% and 20% for the TRC+ 0.25%SCF and TRC+ 0.5%SCF respectively as compared to the TRC 8 L. This is attributed to the stress concentration across these cracks, in addition to the formation of horizontal cracks [49,50]. Figs. 20, 21, and 22 show the crack pattern for the last three tested slabs.

3.6. Mode of failure

The three tested slabs failed in a ductile way with the telescopic failure. Generally, the yarn filaments in the three tested slabs are ruptured partially, especially the two TRC+ 0.25%SCF and TRC+ 0.5%SCF slabs that showed a lower number of ruptured filaments as compared with the TRC tested slab. This is due to the chopped fiber's action in bearing the stresses that transform from the mortar matrix [31,54].

4. Conclusions

1. The carbon fabric reinforcement adds more to the bending strength of TRC slabs than short-distributed fibers with the same volume fraction.
2. The short carbon fibers contribute more to the flexural strength of FRC slabs than they do to the strength of hybrid TRC slabs with the same volume fraction.
3. When the short carbon fibers that makeup 50% and 100% of the carbon fabric volume are added, the two TRC slabs can hold more weight and the load-deflection and load-concrete strain behaviors get better.
4. When short carbon fibers are added, the load that causes cracks is slightly lessened. This is because the random placement of the short fibers limits how stresses can be moved between the fabric reinforcement and the matrix.
5. The addition of the short carbon fibers reduces the compressive strain of the concrete at the crack and increases it at the ultimate load. This is because the short fibers keep the stresses in the compression zone stable during the pre-cracking stage and reduce the strain at the crack's tips during the post-cracking stage. This makes the strain region longer during the multiple cracking stages.

6. By adding the short carbon fibers, the flexural stiffness of the two hybrid TRC slabs after cracking is increased, and the increase in deformation caused by a double load is delayed compared to the conventional TRC slab.

5. Recommendations for future studies

1. The effect of the textile impregnation with the polymers on the overall TRC one-way slab behavior must be investigated. But the polymers mixed with fine sand can be used to study how they affect how well the bond works with the mortar matrix.
2. The bond efficiency must be further investigated. However, the scanning electron microscope (SEM) can spot the TRC microstructure.
3. Using two types of mortar, such as normal mortar and mortar, you can find out how roughness affects the strength of the bond.
4. The use of normal mortar in the TRC members can be investigated.
5. The orientation and geometry of the textile yarns must be investigated.
6. The different effects of increasing and decreasing the thickness of the mortar cover on the TRC's ability to bend must be studied more.
7. The direct combination of the textile reinforcement with the usual steel reinforcement needs to be looked into more in terms of how the stresses are redistributed and how well they work with the stresses in the mortar.

Declaration of Competing Interest

The authors declare that they have no known competing financial interests or personal relationships that could have appeared to influence the work reported in this paper.

Data Availability

No data was used for the research described in the article.

References

[1] H.R. Pakravan, M. Jamshidi, H. Rezaei, Effect of textile surface treatment on the flexural properties of textile-reinforced cementitious composites, J. Ind. Text. 46 (1) (2016) 116–129.
[2] B. Mobasher, Mechanics of Fiber and Textile Reinforced Cement Composites, CRC Press, 2011.
[3] J.M. Illston, P. Domone, Construction Materials: Their Nature and Behaviour, CRC Press, 2001.
[4] S. Qaidi, Y.S. Al-Kamaki, R. Al-Mahaidi, A.S. Mohammed, H.U. Ahmed, O. Zaid, F. Althoey, J. Ahmad, H.F. Isleem, I. Bennetts, Investigation of the effectiveness of CFRP strengthening of concrete made with recycled waste PET fine plastic aggregate, PloS One 17 (7) (2022), e0269664.
[5] K. Charles, D. Suchorski, Reinforcement for concrete materials and application, Acids Educ. Bull. Comm. Mater. Concr. Constr. (2006) E2-00–E-701.
[6] S. Qaidi, H.M. Najm, S.M. Abed, Y.O. Özkılıç, H. Al Dughaishi, M. Alosta, M.M.S. Sabri, F. Alkhatib, A. Milad, Concrete containing waste glass as an environmentally friendly aggregate: a review on fresh and mechanical characteristics, Materials 15 (18) (2022) 6222.
[7] B.A. Tayeh, M.H. Akeed, S. Qaidi, B.H.A. Bakar, Influence of the proportion of materials on the rheology and mechanical strength of ultrahigh-performance concrete, Case Stud. Constr. Mater. 17 (2022), e01433.
[8] A. Saeed, H.M. Najm, A. Hassan, S. Qaidi, M.M.S. Sabri, N.S. Mashaan, A. Comprehensive, Study on the effect of regular and staggered openings on the seismic performance of shear walls, Buildings 12 (9) (2022) 1293.
[9] C.G. Papanicolaou, I.C. Papantoniou, Mechanical behavior of textile reinforced concrete (TRC)/concrete composite elements, J. Adv. Concr. Technol. 8 (1) (2010) 35–47.
[10] R.S. Ravindrarajah, C. Tam, Flexural strength of steel fibre reinforced concrete beams, Int. J. Cem. Compos. Lightweight Concr. 6 (4) (1984) 273–278.
[11] R. Kamani, M. Kamali Dolatabadi, A.A. Jeddi, Flexural design of textile-reinforced concrete (TRC) using warp-knitted fabric with improving fiber performance index (FPI), J. Text. Inst. 109 (4) (2018) 492–500.
[12] A. Peled, B. Mobasher, Pultruded fabric-cement composites, Acids Mater. J. 102 (1) (2005) 15.
[13] M. Tsesarsky, A. Katz, A. Peled, O. Sadot, Textile reinforced concrete (TRC) shells for strengthening and retrofitting of concrete elements: influence of admixtures, Mater. Struct. 48 (1) (2015) 471–484.
[14] R. Barhum, V. Mechtcherine, Influence of short dispersed and short integral glass fibres on the mechanical behaviour of textile-reinforced concrete, Mater. Struct. 46 (4) (2013) 557–572.
[15] M. Hinzen, W. Brameshuber, Influence of matrix composition and short fibres on the workability of fine grained fibre concrete, International RILEM Conference on Material Science; Brameshuber, W., Ed.; RILEM: Aachen, Germany, 2010, pp. 131–140.
[16] B.A. Tayeh, M.H. Akeed, S. Qaidi, B.H.A. Bakar, Influence of microsilica and polypropylene fibers on the fresh and mechanical properties of ultra-high performance geopolymer concrete (UHP-GPC), Case Stud. Constr. Mater. 17 (2022), e01367.
[17] S.M.A. Qaidi, B.A. Tayeh, A.M. Zeyad, A.R.G. de Azevedo, H.U. Ahmed, W. Emad, Recycling of mine tailings for the geopolymers production: a systematic review, Case Stud. Constr. Mater. 16 (2022), e00933.
[18] S.M.A. Qaidi, D. Sulaiman Atrushi, A.S. Mohammed, H. Unis Ahmed, R.H. Faraj, W. Emad, B.A. Tayeh, H. Mohammed Najm, Ultra-high-performance geopolymer concrete: A review, Constr. Build. Mater. 346 (2022), 128495.
[19] M. El Kadi, L. Nahum, A. Peled, T. Tysmans, Layered Finite Element (FE) modelling of structural concrete beams non-uniformly reinforced with carbon textile fabrics, Mater. Struct. 54 (5) (2021) 1–13.
[20] M.H. Akeed, S. Qaidi, H.U. Ahmed, R.H. Faraj, A.S. Mohammed, W. Emad, B.A. Tayeh, A.R.G. Azevedo, Ultra-high-performance fiber-reinforced concrete. Part IV: Durability properties, cost assessment, applications, and challenges, Case Stud. Constr. Mater. 17 (2022), e01271.
[21] M.H. Akeed, S. Qaidi, H.U. Ahmed, R.H. Faraj, A.S. Mohammed, W. Emad, B.A. Tayeh, A.R.G. Azevedo, Ultra-high-performance fiber-reinforced concrete. Part I: Developments, principles, raw materials, Case Stud. Constr. Mater. 17 (2022), e01290.
[22] M.H. Akeed, S. Qaidi, H.U. Ahmed, R.H. Faraj, A.S. Mohammed, W. Emad, B.A. Tayeh, A.R.G. Azevedo, Ultra-high-performance fiber-reinforced concrete. Part II: Hydration and microstructure, Case Stud. Constr. Mater. 17 (2022), e01289.
[23] M.H. Akeed, S. Qaidi, H.U. Ahmed, R.H. Faraj, S.S. Majeed, A.S. Mohammed, W. Emad, B.A. Tayeh, A.R.G. Azevedo, Ultra-high-performance fiber-reinforced concrete. Part V: Mixture design, preparation, mixing, casting, and curing, Case Stud. Constr. Mater. 17 (2022), e01363.
[24] M.H. Akeed, S. Qaidi, H.U. Ahmed, W. Emad, R.H. Faraj, A.S. Mohammed, B.A. Tayeh, A.R.G. Azevedo, Ultra-high-performance fiber-reinforced concrete. Part III: fresh and hardened properties, Case Stud. Constr. Mater. 17 (2022), e01265.

[25] T.D. Hrynyk, F.J. Vecchio, Behavior of steel fiber-reinforced concrete slabs under impact load, Struct. J. 111 (5) (2014) 1213–1224.
[26] I.Y. Hakeem, M. Amin, B.A. Abdelsalam, B.A. Tayeh, F. Althoey, I.S. Agwa, Effects of nano-silica and micro-steel fiber on the engineering properties of ultra-high performance concrete, Struct. Eng. Mech. 82 (3) (2022) 295–312.
[27] S. Yildizel, Material properties of basalt-fiber-reinforced gypsum-based composites made with metakaolin and silica sand, Mech. Compos. Mater. 56 (3) (2020) 379–388.
[28] S. Yildizel, O. Timur, A. Ozturk, Abrasion resistance and mechanical properties of waste-glass-fiber-reinforced roller-compacted concrete, Mech. Compos. Mater. 54 (2) (2018) 251–256.
[29] Y.I.A. Aisheh, D.S. Atrushi, M.H. Akeed, S. Qaidi, B.A. Tayeh, Influence of polypropylene and steel fibers on the mechanical properties of ultra-high-performance fiber-reinforced geopolymer concrete, Case Stud. Constr. Mater. 17 (2022), e01234.
[30] Y.I.A. Aisheh, D.S. Atrushi, M.H. Akeed, S. Qaidi, B.A. Tayeh, Influence of steel fibers and microsilica on the mechanical properties of ultra-high-performance geopolymer concrete (UHP-GPC), Case Stud. Constr. Mater. 17 (2022), e01245.
[31] A.M. Zeyad, A.H. Khan, B.A. Tayeh, Durability and strength characteristics of high-strength concrete incorporated with volcanic pumice powder and polypropylene fibers, J. Mater. Res. Technol. 9 (1) (2020) 806–818.
[32] M. Amin, I.Y. Hakeem, A.M. Zeyad, B.A. Tayeh, A.M. Maglad, I.S. Agwa, Influence of recycled aggregates and carbon nanofibres on properties of ultra-high-performance concrete under elevated temperatures, Case Stud. Constr. Mater. 16 (2022), e01063.
[33] S.M.A. Qaidi, B.A. Tayeh, H.F. Isleem, A.R.G. de Azevedo, H.U. Ahmed, W. Emad, Sustainable utilization of red mud waste (bauxite residue) and slag for the production of geopolymer composites: A review, Case Stud. Constr. Mater. 16 (2022), e00994.
[34] S.M.A. Qaidi, B.A. Tayeh, H.U. Ahmed, W. Emad, A review of the sustainable utilisation of red mud and fly ash for the production of geopolymer composites, Constr. Build. Mater. 350 (2022), 128892.
[35] S.M.A. Qaidi, A.S. Mohammed, H.U. Ahmed, R.H. Faraj, W. Emad, B.A. Tayeh, F. Althoey, O. Zaid, N.H. Sor, Rubberized geopolymer composites: a comprehensive review, Ceram. Int. 48 (17) (2022) 24234–24259.
[36] G. Calis, M.E. Akpinar, S.A. Yildizel, M.T. Çöğürcü, Evaluation and optimization Of PVA reinforced cementitious composite containing metakaolin and fly ash, Rev. Romana De. Mater. 51 (1) (2021) 53–66.
[37] Z. Saidova, G. Yakovlev, O. Smirnova, A. Gordina, N. Kuzmina, Modification of cement matrix with complex additive based on chrysotyl nanofibers and carbon black, Appl. Sci. 11 (15) (2021) 6943.
[38] E.-B. Jeon, S. Ahn, I.-G. Lee, H.-I. Koh, J. Park, H.-S. Kim, Investigation of mechanical/dynamic properties of carbon fiber reinforced polymer concrete for low noise railway slab, Compos. Struct. 134 (2015) 27–35.
[39] O. Smirnova, Rheologically active microfillers for precast concrete, Int. J. Civ. Eng. Technol. 9 (8) (2018) 1724–1732.
[40] O. Smirnova, Technology of increase of nanoscale pores volume in protective cement matrix, Int. J. Civ. Eng. Technol. 9 (10) (2018) 1991–2000.
[41] O. Smirnova, Low-Clinker cements with low water demand, J. Mater. Civ. Eng. 32 (7) (2020), 06020008.
[42] C.-C. Chen, S.-L. Chen, Strengthening of reinforced concrete slab-column connections with carbon fiber reinforced polymer laminates, Appl. Sci. 10 (1) (2019) 265.
[43] V. Kodur, L.A. Bisby, Evaluation of fire endurance of concrete slabs reinforced with fiber-reinforced polymer bars, J. Struct. Eng. 131 (1) (2005) 34–43.
[44] O.H. Hussien, A.M. Ibrahim, S.M. Abd, Improving Flexural Behavior of Textile Reinforced Concrete One Way Slab by Removing Weft Yarns with Different Percentages, Civ. Eng. J. 4 (12) (2018) 2903–2918.
[45] Y. Du, X. Zhang, L. Liu, F. Zhou, D. Zhu, W. Pan, Flexural behaviour of carbon textile-reinforced concrete with prestress and steel fibres, Polymers 10 (1) (2018) 98.
[46] H.R. Pakravan, T. Ozbakkaloglu, Synthetic fibers for cementitious composites: a critical and in-depth review of recent advances, Constr. Build. Mater. 207 (2019) 491–518.
[47] K. Abdelsamie, I.S. Agwa, B.A. Tayeh, R.D.A. Hafez, Improving the brittle behaviour of high-strength concrete using keratin and glass fibres, Adv. Concr. Constr. 12 (6) (2021) 469–477.
[48] O.Z. Jaradat, K. Gadri, B.A. Tayeh, A. Guettalaa, Influence of sisal fibres and rubber latex on the engineering properties of sand concrete, Struct. Eng. Mech. 80 (1) (2021) 47–62.
[49] S. Fares, R. Fugger, S. De Santis, G. de Felice, Strength, bond and durability of stainless steel reinforced grout, Constr. Build. Mater. 322 (2022), 126465.
[50] C. Signorini, A. Nobili, Comparing durability of steel reinforced grout (SRG) and textile reinforced mortar (TRM) for structural retrofitting, Mater. Struct. 54 (3) (2021) 1–15.
[51] R. Barhum, V. Mechtcherine, Effect of short, dispersed glass and carbon fibres on the behaviour of textile-reinforced concrete under tensile loading, Eng. Fract. Mech. 92 (2012) 56–71.
[52] H.M. Najm, O. Nanayakkara, M.M.S. Sabri, Destructive and non-destructive evaluation of fibre-reinforced concrete: a comprehensive study of mechanical properties, Materials 15 (13) (2022) 4432.
[53] C. Design, Construction of building structures with fibre-reinforced polymers, Can. Stand. Assoc. Missisauga (2012) 28.
[54] A.-A. Alyaa A, A. Mazin B, H. Hussein M, T. Bassam A, Investigating the behaviour of hybrid fibre-reinforced reactive powder concrete beams after exposure to elevated temperatures, J. Mater. Res. Technol. 9 (2) (2020).